Precision tests of QCD with jets and vector bosons at HERA and TevaTron

C. Glasman
Universidad Autónoma de Madrid, Spain

Recent results from HERA and TevaTron on precision tests of QCD with jets, W and Z bosons and photons associated with jets and heavy flavours are presented. The measurements were used to probe QCD at the highest energies, to provide experimental constraints on SM processes that constitute background to new physics, to extract values of the coupling of the strong interaction and to constrain the proton parton distribution functions. The implications of the results on LHC physics are discussed.

1. Introduction

Parton-parton scattering via QCD interactions is the main process at hadron colliders. Besides their intrinsic interest, these processes represent sometimes an irreducible background to other Standard Model (SM) processes and to new physics.

The ep collider HERA, which provides a simple hadronic enviroment to test QCD, and the $p\bar{p}$ collider TevaTron, which provides the highest available energies, have produced over the years complementary precision measurements of the parameters of the theory and precise tests of its underlying dynamics. All this knowledge will be crucial for understanding any physics at LHC. For instance, the gluon density at low x is a necessary input ingredient for calculating the Higgs production cross section, whereas the predictions for W or Z bosons production cross sections require knowledge of the quark densities.

This report summarises the most recent results from jet cross sections, forward jets, photons and W and Z bosons and the underlying event presented by the CDF, DØ, H1 and ZEUS experiments at ICHEP08.

2. Studies of the underlying event

The main experimental uncertainties for jet cross sections arise from the jet energy scale and the underlying event (UE), which contributes with additional energy density on top of the hard interaction but is not related to it; this is a non-perturbative effect which is not included in the calculations. These effects can be simulated with Monte Carlo simulations and are extremely model dependent, so a good understanding of the UE at the available energies is crucial to model its effects at LHC energies.

The CDF collaboration has performed a new study of the UE using Drell-Yan processes [1]. In this analysis, all particles in the final state, except the lepton pair, can be considered as the UE. Thus, the Drell-Yan events constitute a very clean probe of the UE. The study of the UE observables was done for lepton-pair masses around that of the Z boson ($70 < M_{l\bar{l}} < 110$ GeV). The transverse plane was separated in four regions: the toward region, which corresponds to the Z-boson direction, the opposite direction, which is called the away region, and the two transverse regions. The transverse regions are most sensitive to the UE. Several observables, such as the charged particle density shown in Fig. 1a, were studied as functions of the transverse momentum of the lepton pair. The measurements are approximately constant for the transverse and toward regions and increase with lepton-pair p_T in the away region. The PYTHIA tune AW MC predictions describe very well the data. Figure 1b shows the comparison of the UE observables in Drell-Yan events with the same observable for the leading-jet analysis in the transverse region. The results are in good agreement so the Drell-Yan studies provide insight into the UE in a cleaner environment.

Photoproduction at HERA also allows the study of the UE. At leading order (LO), there are two processes that contribute to jet photoproduction: direct, in which the photon interacts as a point-like particle with the partons from the proton, and resolved, in which the photon interacts via its partonic structure, giving rise to a hadronic-like final state. The observable $x_\gamma^{\rm obs} = (1/E_\gamma)(\sum_{\rm jets} E_T^{\rm jet} e^{-\eta^{\rm jet}})$, where $E_T^{\rm jet}$ is the jet transverse energy, $\eta^{\rm jet}$ is the jet

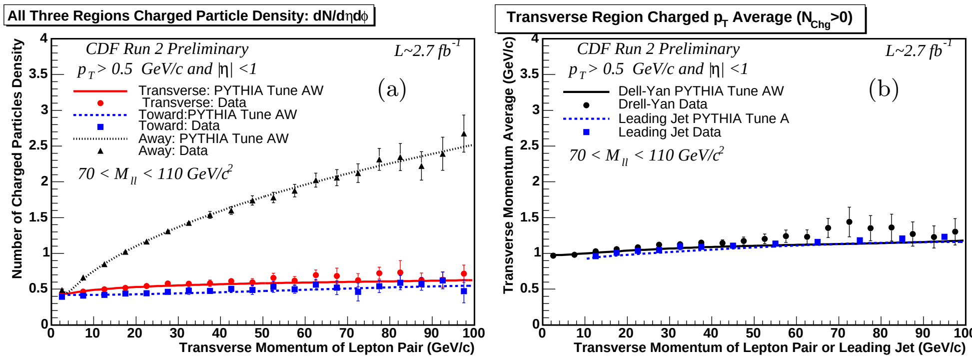

Figure 1: (a) Charged particle density vs. transverse momentum of lepton pair; (b) transverse momentum average vs. transverse momentum of lepton pair or leading jet.

pseudorapidity and E_γ is the energy of the incoming photon, measures the fraction of the photon energy invested in the hard interaction and can be used to separate both contributions since direct processes take high values of $x_\gamma^{\rm obs}$, whereas resolved processes take smaller values. Measurements of multijet production in photoproduction are directly sensitive to high orders and can be used to test the parton-shower models. Resolved processes allow tests of multiparton interactions and the UE. The UE has been studied at HERA using dijet events in photoproduction. Jet profiles have been measured [2] by the H1 Collaboration in terms of the mean charged multiplicity as a function of the azimuthal angle, separately for $x_\gamma^{\rm obs} < 0.7$, dominated by resolved processes, and $x_\gamma^{\rm obs} > 0.7$, dominated by direct (see Fig. 2a and b). For $x_\gamma^{\rm obs} < 0.7$, a significant contribution from the UE is expected. The mean charged multiplicity has also been measured as a function of the leading-jet $E_T^{\rm jet}$ for $x_\gamma^{\rm obs} < 0.7$ in four regions of ϕ (see Fig. 2c, d, e and f). The mean charged multiplicity increases with increasing $E_T^{\rm jet}$ in the toward and away regions and decreases in the transverse regions. The inclusion of multiparton interactions (MPIs) in the PYTHIA MC prediction improves the description of the data in all four regions. The ZEUS Collaboration has measured [3] the three-jet cross section in photoproduction as a function of $x_\gamma^{\rm obs}$ for invariant masses below 50 GeV. The measurement is shown in Fig. 3a and displays a two-peak structure at low and high $x_\gamma^{\rm obs}$ values, which can be identified with the resolved and direct processes, respectively. Figure 3b shows the four-jet invariant mass cross section. The data are compared with the predictions of PYTHIA and HERWIG MC models with and without MPIs; the models without MPIs describe the data at high invariant mass for all $x_\gamma^{\rm obs}$ values, but fail at low invariant mass and low $x_\gamma^{\rm obs}$. The models which include MPIs give an improved description of the data at low $x_\gamma^{\rm obs}$ and low mass.

3. Probing QCD at the highest energies

The CDF [4] and the DØ [5] Collaborations have measured the inclusive-jet cross section in $p\bar{p}$ collisions at $\sqrt{s} = 1.96$ TeV as a function of $E_T^{\rm jet}$ for different regions of rapidity using the mid-point jet algorithm (see Fig. 4). These are high precision measurements, especially at high $E_T^{\rm jet}$, where new physics might show up. These cross sections are also sensitive to the gluon density at high x. The next-to-leading-order (NLO) QCD calculations give a good description of the data. These measurements constitute the most stringent test of pQCD at the highest available energies so far.

Jet production provides the highest energy reach with highest statistics. In particular, dijet production is ideal to test the SM and search for new physics, which might show up as narrow resonances in the dijet invariant mass spectrum. Figures 5a and 5b show the measurement of the dijet invariant mass from CDF [4]; the data reach values of up to 1.4 TeV, which constitute the highest energies measured so far. The NLO calculations give a good description of the data in the whole measured range. Since no evidence for new physics is observed, 95% CL limits were set for various models, which include excited quarks, new heavy vector bosons and gravitons. Figure 5c and 5d show the limits obtained from the data as functions of the new particle mass.

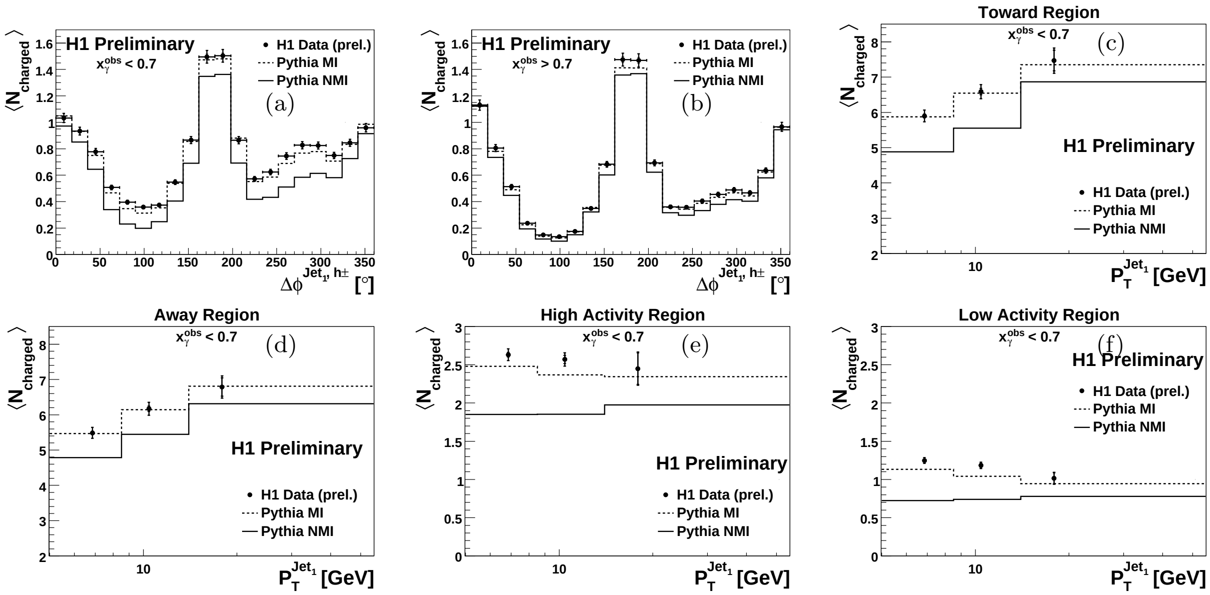

Figure 2: Mean charged multiplicity as a function of $\Delta\phi^{\rm jet}$ for (a) $x_\gamma^{\rm obs} < 0.7$ and (b) $x_\gamma^{\rm obs} > 0.7$; mean charged multiplicity as a function of $p_T^{\rm jet}$ in the (c) toward, (d) away, (e) high-activity and (f) low-activity regions.

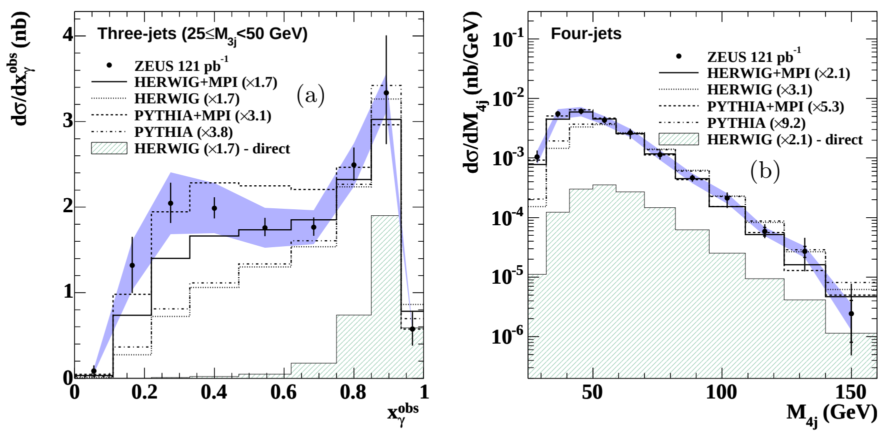

Figure 3: (a) Three-jet cross section as a function of $x_\gamma^{\rm obs}$; (b) four-jet cross section as a function of the four-jet invariant mass.

Angular correlations in the dijet system are directly sensitive to the underlying parton dynamics and can also be used to search for new physics. The angular correlation, defined as $\chi_{\rm dijets} = \exp(|y_1 - y_2|)$, is expected to be constant for Rutherford scattering; QCD processes induce a small deviation from this behaviour, but new physics is expected to have a very different shape at low values of $\chi_{\rm dijets}$. The DØ Collaboration has measured [6] $\chi_{\rm dijets}$ in different regions of dijet invariant mass from 0.25 to above 1.1 TeV, as shown in Fig. 6a. The NLO predictions give a good description of the data in the whole measured range. Since there is no indication for the presence of new physics, 95% CL limits were set for various models which include quark compositeness and extra dimensions. Figures 6b, 6c and 6d show the χ^2, likelihood and probability as a function of the characteristic parameter of each model. These constitute the most stringent limits for these models from hadron colliders up to date.

4. Precision tests of QCD

Recently, very precise measurements of jet cross sections in neutral current (NC) DIS and photoproduction, which are directly sensitive to the gluon content of the proton, have been incorporated in a QCD fit to determine the proton PDFs. The result was an improved determination of the gluon density for mid- to high-x values, a region relevant for new physics searches at LHC. In some regions of phase space the uncertainty in the gluon density

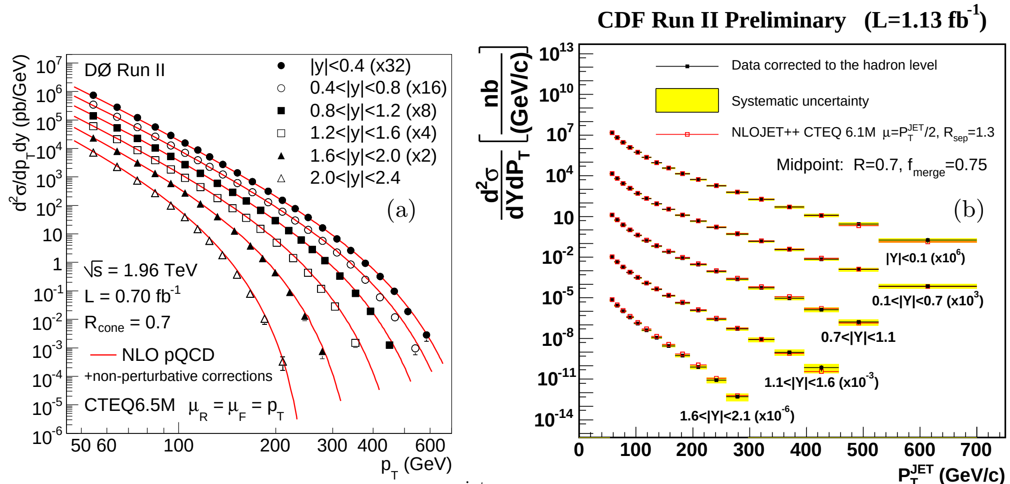

Figure 4: Inclusive-jet cross sections as functions of $E_T^{\rm jet}$ in different rapidity regions measured by (a) DØ and (b) CDF.

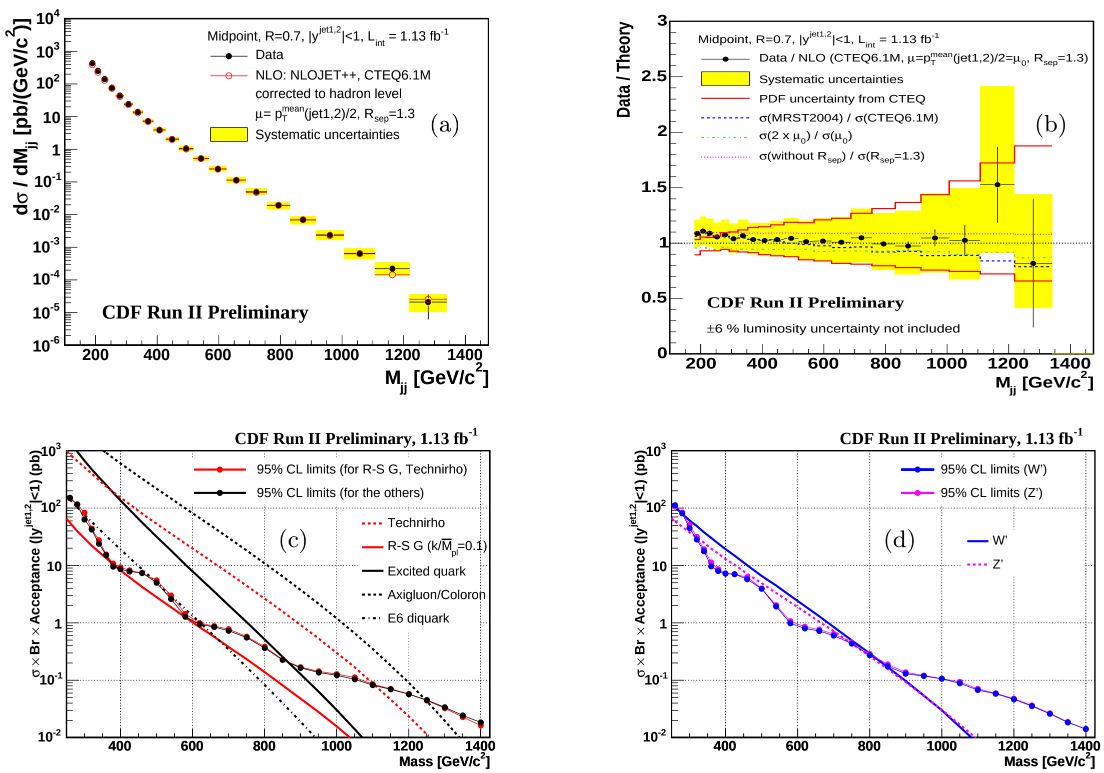

Figure 5: (a,b) Dijet invariant mass cross section; (c,d) 95% CL limits as functions of the particle mass.

decreased by up to a factor of two. Now the H1 and ZEUS Collaborations are making new and more precise jet measurements with full HERA luminosity and extended phase space to take full advantage of this technique. The ZEUS Collaboration has measured double-differential dijet cross sections in NC DIS [7] and photoproduction [8] as functions of $\xi = x_{\rm Bj}(1 + M_{\rm jj}^2/Q^2)$ and $x_p^{\rm obs} = (1/2E_p)(\sum_{\rm jets} E_T^{\rm jet} e^{\eta^{\rm jet}})$, respectively, which are both estimators of the fractional momentum carried by the struck parton. The measurements are shown in Fig. 7 and are well described by the NLO calculations. These analyses provide a stringent test of QCD and were optimised to obtain the best sensitivity to the gluon density in the proton.

Inclusive-jet cross sections in charged current DIS have been measured [9] by the ZEUS Collaboration. Figure 8a shows the cross section as a function of x for electron beams (sensitive to the u-quark density) and positron beams (sensitive to the d-quark density). The NLO calculations give a good description of the data. Figure 8b shows the

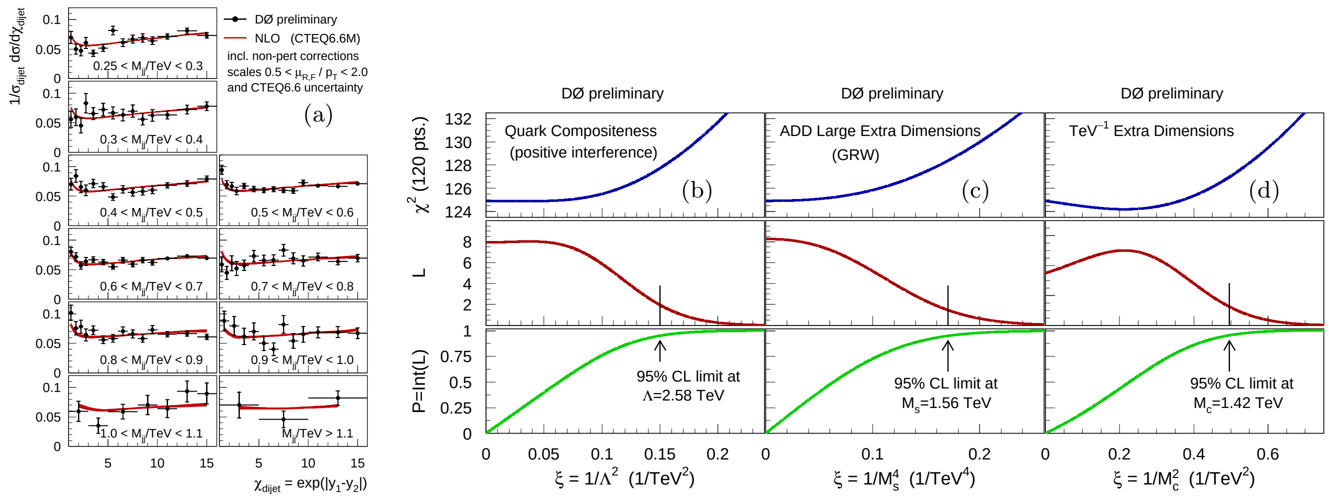

Figure 6: (a) Dijet cross sections as functions of $\chi_{\rm dijets}$; (b,c,d) χ^2, likelihood and probability as functions of the characteristic parameter of each model.

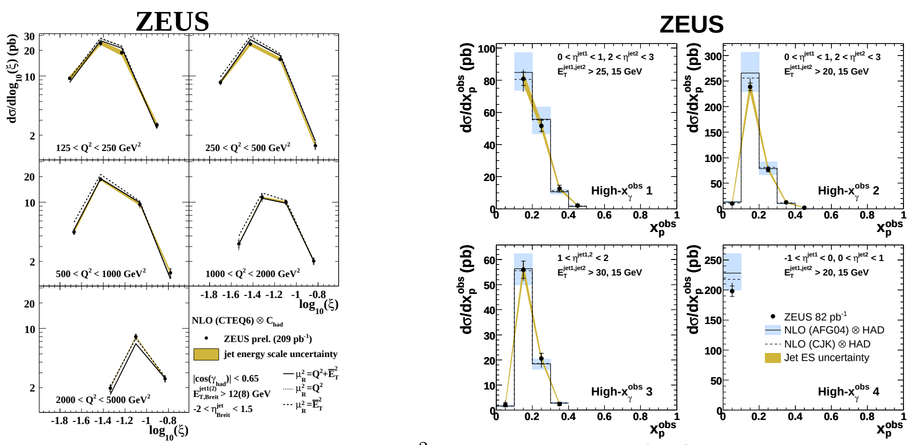

Figure 7: Dijet cross sections as functions of ξ in different Q^2 regions in NC DIS (left); dijet cross sections as functions of $x_p^{\rm obs}$ in photoproduction (right).

theoretical uncertainties, clearly dominated by the PDF uncertainty, which is largest for positron beams at high x. Therefore, these measurements have the potential to constrain further the valence-quark PDFs if included in global fits.

Inclusive-jet cross sections in NC DIS were measured [10] by the H1 Collaboration as a function of $E_T^{\rm jet}$ in different regions of Q^2 in the range $5 < Q^2 < 100$ GeV^2 (see Fig. 9a). The NLO predictions give a good description of the data. However, the theoretical uncertainty, which is dominated by terms beyond NLO, is large: it reaches up to 30% at the lowest Q^2 values. This shows the need for higher-order corrections. These measurements can help to constrain the gluon PDF at low Q^2 (low x) when higher-order calculations become available for NC DIS.

4.1. Precision measurements of α_s

The success of pQCD lies on the precise and consistent determinations of α_s from many diverse phenomena, such as structure functions, τ decays, Z-line shape, lattice, jets, etc. At HERA, many determinations of α_s, mostly extracted from jet observables, give values as precise as those from more inclusive measurements. The H1 and ZEUS Collaborations have made new determinations of α_s, focusing on decreasing the uncertainties further. The H1 Collaboration has determined [10, 13] these values of α_s: $\alpha_s(M_Z) = 0.1186 \pm 0.0014({\rm exp.}) \pm 0.0134({\rm th.})$ and $\alpha_s(M_Z) = 0.1196 \pm 0.0010({\rm exp.}) \pm 0.0053({\rm th.})$ from the inclusive-jet cross sections at low Q^2 and the normalised inclusive-jet cross sections (see Fig. 9b) in the regions $5 < Q^2 < 100$ GeV^2 and $150 < Q^2 < 15000$ GeV^2, respectively.

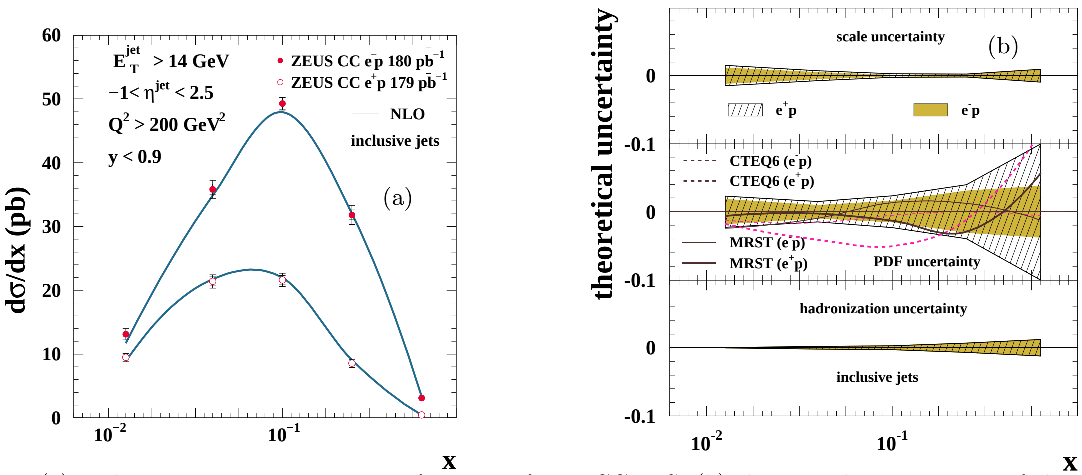

Figure 8: (a) Inclusive-jet cross section as a function of x in CC DIS; (b) theoretical uncertainties of the inclusive-jet cross-section prediction as a function of x in CC DIS.

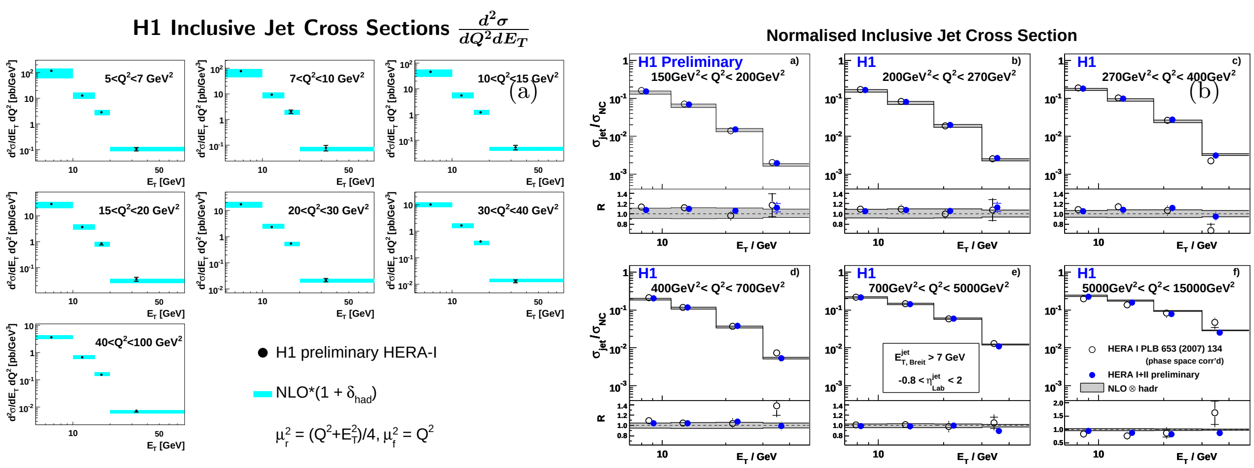

Figure 9: Inclusive-jet cross sections as functions of E_T^{jet} in different regions of Q^2 in NC DIS.

In this way, a region of phase space was selected in which experimental uncertainties are well under control and also, the use of normalised cross sections yields a cancellation of correlated uncertainties. New determinations of α_s were performed by ZEUS from the inclusive-jet cross sections in NC DIS [11] and photoproduction [12] at high Q^2 and high E_T^{jet}, respectively, where the theoretical uncertainties are minimised. Figure 10a shows the cross section in NC DIS as a function of Q^2 for different values of the jet-radius parameter R in the k_T algorithm. The NLO calculations give a good description of the data for $R = 0.5 - 1.0$ with similar accuracy. Figure 10b shows the cross section as a function of E_T^{jet} in photoproduction; the NLO calculation also gives a good description of the data for these processes. Values of α_s were extracted from these measurements: $\alpha_s(M_Z) = 0.1207 \pm 0.0014(\text{stat.})^{+0.0035}_{-0.0033}(\text{syst.})^{+0.0022}_{-0.0023}(\text{th.})$ (NC DIS, $Q^2 > 500$ GeV^2) and $\alpha_s(M_Z) = 0.1223 \pm 0.0001(\text{stat.})^{+0.0023}_{-0.0021}(\text{syst.}) \pm 0.0030(\text{th.})$ (photoproduction, $E_T^{jet} > 17$ GeV).

To reduce the uncertainties even further and to take advantage of the cross-calibration between experiments, a simultaneous fit to the inclusive-jet cross sections in NC DIS from H1 and ZEUS has been performed [14] to give

$$\alpha_s(M_Z) = 0.1198 \pm 0.0019\ (\text{exp.}) \pm 0.0026\ (\text{th.}).$$

The total uncertainty of the combined value, ±2.7%, is very competitive with the most recent result from LEP.

5. Probing QCD with vector bosons

Production of isolated photons in $p\bar{p}$ collisions at TeVatron are a probe of QCD dynamics. Photons coming directly from the hard interaction are largely independent of hadronisation corrections. The understanding of these processes

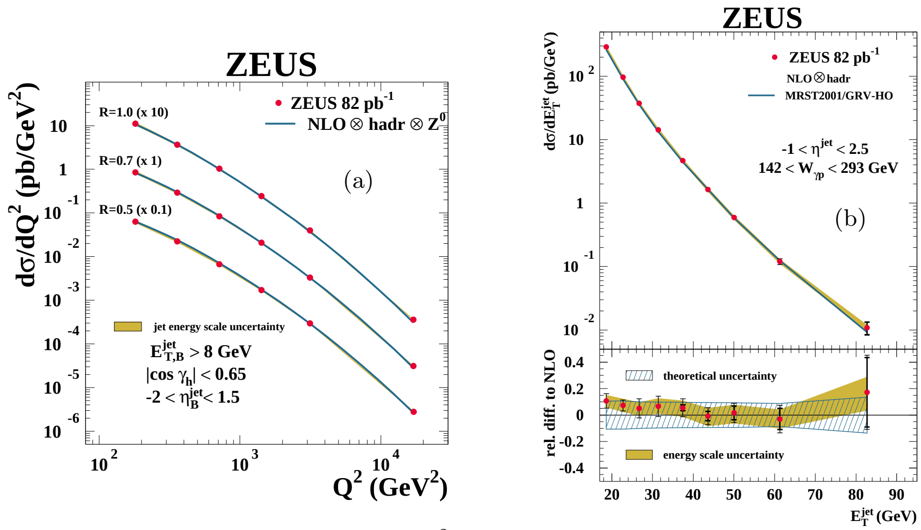

Figure 10: (a) Inclusive-jet cross sections as functions of Q^2 for different values of the jet radius R in NC DIS; (b) inclusive-jet cross section as a function of $E_T^{\rm jet}$ in photoproduction.

in QCD is crucial for searches of new particles that decay into photons. The CDF Collaboration has measured [15] the inclusive cross section for isolated photons as a function of the photon transverse momentum integrated over the photon rapidity range $|\eta^\gamma| < 1$. Figure 11a shows the measurement together with the NLO predictions. The calculations describe the data adequately within the experimental and theoretical uncertainties.

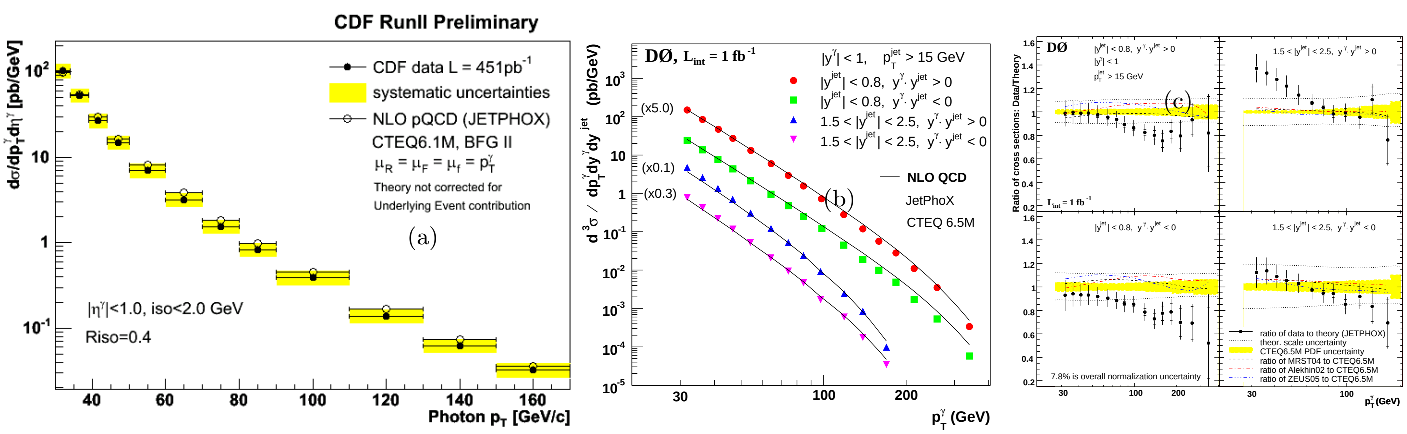

Figure 11: (a) Isolated-photon cross section as a function of the photon p_T; (b,c) isolated-photon plus jet cross sections as functions of photon p_T for different configurations of photon and jet rapidities.

The DØ Collaboration has studied [16] in more detail these processes by measuring the cross section of isolated photons in association with jets. The measurements were done as functions of the photon transverse momentum for different configurations of photon and jet rapidities. These measurements have the potential to constrain the proton PDFs and different angular configurations give access to different regions of Q^2 and x. Figures 11b and c show the measurements together with the NLO calculations. The NLO predictions, using different sets of proton PDFs can not describe the shape of the cross sections simultaneously over the entire range measured. Therefore, the theoretical understanding of these processes needs to be improved before these data can be used to constrain the proton PDFs.

Inclusive prompt photons and in association with jets have been measured at HERA in photoproduction by the H1 Collaboration [17]. These processes are sensitive to the PDFs both in the proton and the photon. Inclusive prompt photon production has been measured as a function of the transverse energy and pseudorapidity of the photon (see Figs. 12a and 12b). The NLO calculations are below the data, especially at low E_T^γ and low η^γ. The production of isolated photons in association with jets has been measured as a function of E_T^γ, η^γ and $x_\gamma^{\rm obs}$ (see Figs. 12c to 12e).

The NLO calculations give a better description of these data than for inclusive photons, except at high $x_\gamma^{\rm obs}$.

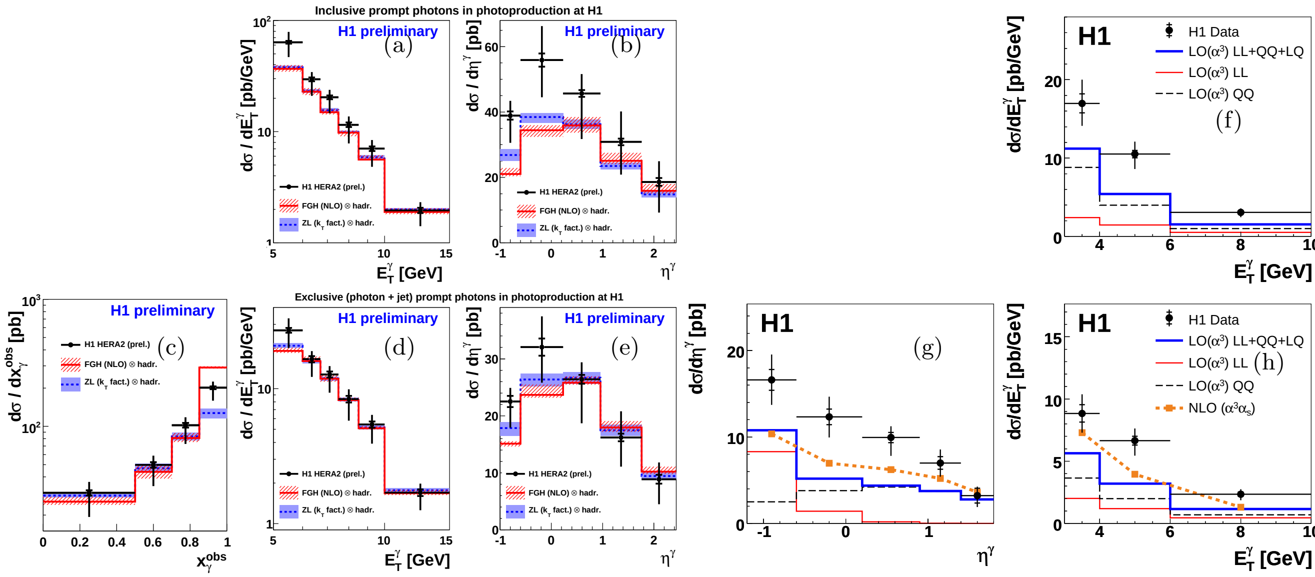

Figure 12: Inclusive-photon cross sections as functions of (a) E_T^γ and (b) η^γ in photoproduction; exclusive-photon cross sections as functions of (c) $x_\gamma^{\rm obs}$, (b) E_T^γ and (c) η^γ in photoproduction; (f) inclusive-photon cross section as a function of E_T^γ in NC DIS; exclusive-photon cross sections as functions of (g) η^γ and (h) E_T^γ in NC DIS.

Isolated photons have also been measured [18] in NC DIS by the H1 Collaboration. In this case, there are two major contributions to photon emission, from the lepton and from the quark lines. The measurements have been performed inclusively and in association with jets as functions of photon transverse energy and pseudorapidity (see Figs. 12f, g and h). The LO calculations describe the shape of the data but underestimate the normalisation by a factor of approximately two, which can be attributed to an underestimation of the quark-line contribution. The NLO calculations, which are only available for photons in association with jets in this process, are higher than the LO predictions, but still below the data. Therefore, the theoretical understanding of these processes needs to be improved.

The production of vector bosons in association with jets in $p\bar{p}$ collisions is a key channel for studying top production within the SM as well as for searches of Higgs and new physics. The study of the production via QCD processes also provides a stringent test of the theory. The CDF and DØ Collaborations have measured the production of W [19] and Z [20] bosons in association with jets. Figure 13a shows the measurements of W+jets from CDF, as a function of $E_T^{\rm jet}$ of the first, second and third jets, and Fig. 13b shows the measurement of Z+jets from DØ, as a function of $E_T^{\rm jet}$. The pQCD calculations, which are NLO for up to two jets, are compared with the measurements. The NLO calculations give a good description of the total and differential cross sections.

$W + c$-jet production at TevaTron is dominated by the s-gluon fusion channel and so is sensitive to the $V_{\rm cs}$ matrix element. The measurements are also sensitive to the s and g PDFs. This process constitutes a background to top, Higgs and stop production as well as to other searches for new physics. The DØ Collaboration has measured [21] the total fraction of $W + c$-jet to W+jets, $\frac{\sigma(W+c-{\rm jet})}{\sigma(W+{\rm jets})}$, to be $0.074 \pm 0.019({\rm stat.})^{+0.012}_{-0.014}({\rm syst.})$, as well as differentially as a function of $E_T^{\rm jet}$ (see Fig. 14a). The CDF Collaboration has measured [22] the total cross section times the branching ratio of the $W \to l\nu$ channel, $\sigma_{W+c-{\rm jet}} \times Br(W \to l\nu) = 9.8 \pm 3.2$ pb. Figures 14b and 14c show the distributions of the difference between same-sign and opposite-sign events as a function of the lepton p_T, which shows clearly the signal. The predictions are in reasonable agreement with the data. These measurements provide a direct experimental evidence for the signal and constitute an experimental validation of the $W + c$ theoretical prediction for use in searches.

$W + b$-jet and $Z + b$-jet production are also important backgrounds to Higgs searches and are sensitive to the b parton density needed to predict the production of Higgs, SUSY, top and other new particles. The CDF Collaboration

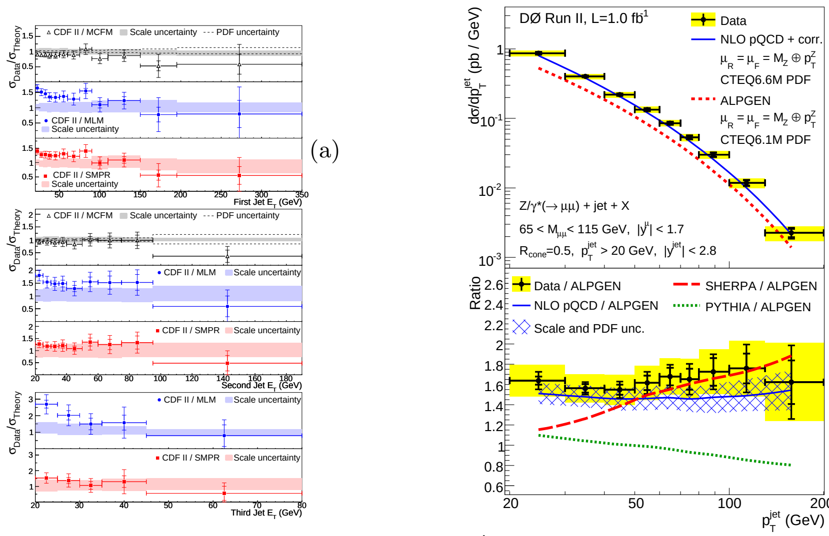

Figure 13: (a) W+jets cross sections as functions of $E_T^{\rm jet}$; (b) Z+jets cross section as a function of $E_T^{\rm jet}$.

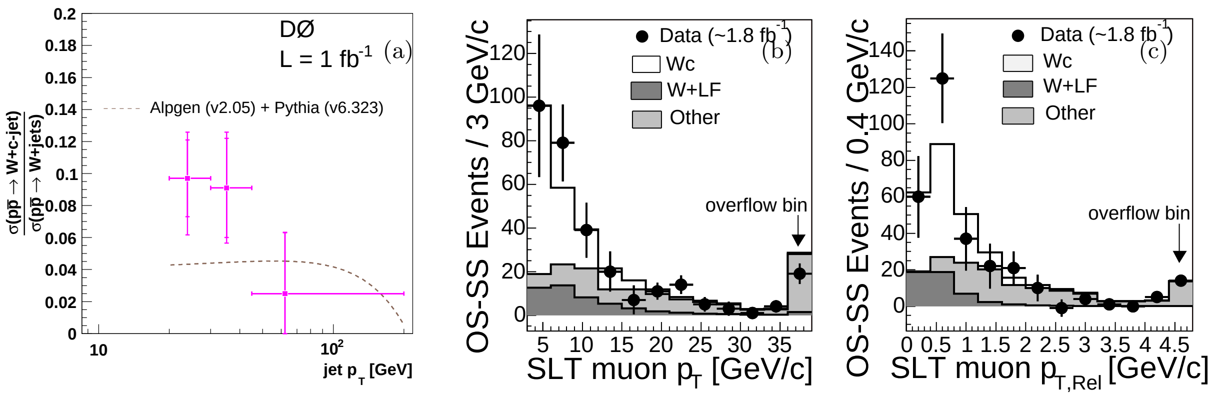

Figure 14: (a) Ratio of the $\sigma(W+c-\text{jet})$ to $\sigma(W+\text{jets})$; (b) muon p_T and $p_{T,\text{rel}}$ distributions.

has measured [23] the total cross sections for $W+b$-jet and $Z+b$-jet production, $\sigma(Z{+}b-\text{jet}) = 0.86 \pm 0.14 \pm 0.12$ pb and $\sigma(W{+}b-\text{jet}) \times BR(W \to l\nu) = 2.74 \pm 0.27 \pm 0.42$ pb. The predictions are 0.53 pb (NLO) and 0.78 pb (Alpgen), respectively. The measured $\sigma(Z{+}b-\text{jet})$ cross section is somewhat higher than the NLO prediction. The normalised differential cross sections as functions of $E_T^{\rm jet}$ and p_T^Z show that the predictions fall below the data at low values but describe the data well at high $E_T^{\rm jet}$ and high p_T^Z (see Fig. 15). For $W+b$-jet production, the LO prediction is about 3.5 times lower than the data. The calculation has an uncertainty of $30-40\%$, whereas the data has an uncertainty of only 18%, so these measurements should be very helpful to constrain the theory.

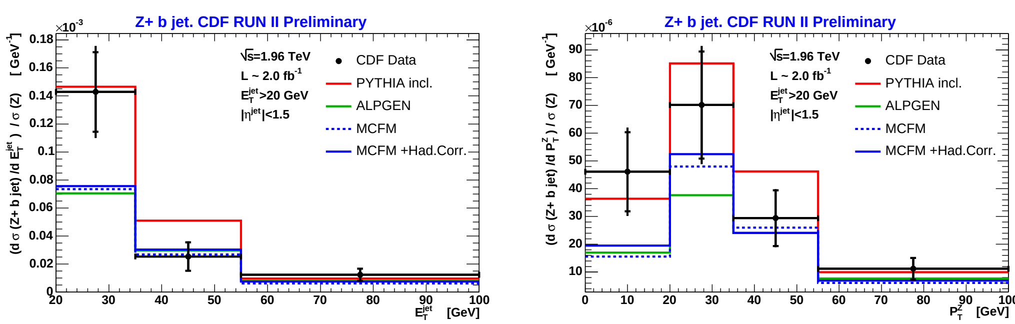

Figure 15: Normalised $Z+b$-jet cross sections as functions of $E_T^{\rm jet}$ (left) and p_T^Z (right).

The production of photons in association with b- or c-jets also provides a test of QCD. The DØ Collaboration has measured [24] the cross sections for photons plus b- or c-jets as functions of the photon transverse energy in different rapidity configurations. Figure 16 shows the measurements together with the NLO calculations. The predictions are in good agreement with the data for photon+b-jets in all the E_T^γ range and for photon+c-jets for $E_T^\gamma < 50$ GeV. The disagreement between the photon+c measurements and the theory is seen to grow with increasing E_T^γ. The origin of this discrepancy is not yet clear; it could be attributed, for instance, to intrinsic charm in the proton or to uncertainties in the splitting of gluons into heavy-quark pairs.

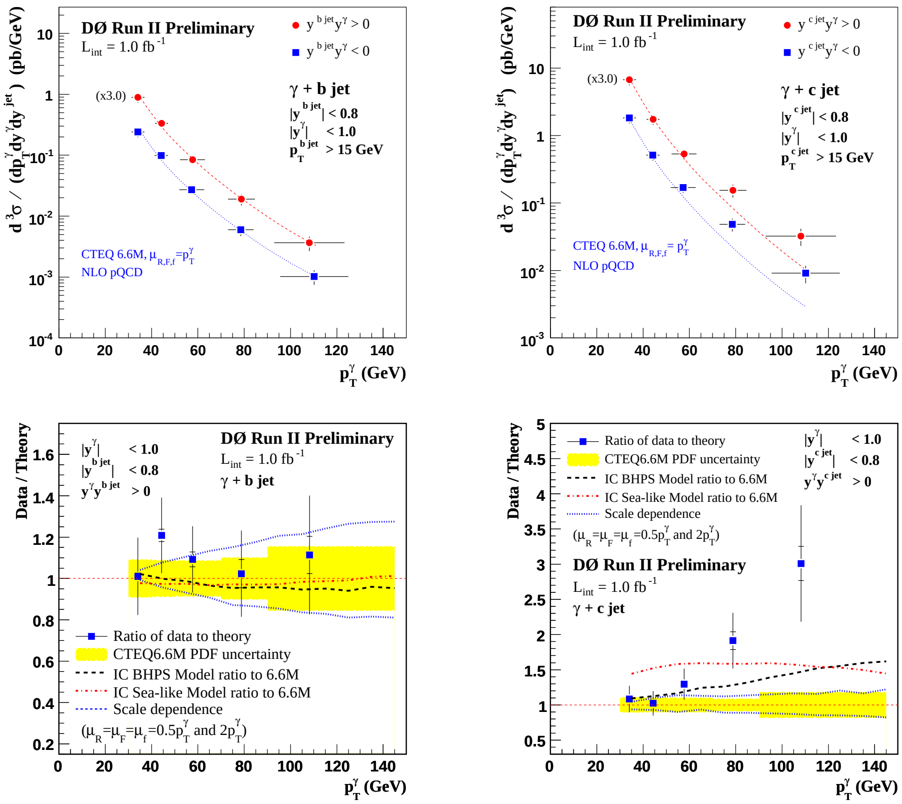

Figure 16: Photon+b-jets (left) and photon+c-jets (right) cross sections as functions of p_T^γ.

6. Parton dynamics at low x

One of the main channels of Higgs production at LHC is $gg \to H$ via a top-quark loop. The predictions for this process need information on the parton evolution at low x. This information can be obtained from low-x jet data at HERA. At high scales, calculations at NLO using DGLAP evolution give a good description of the data. However, DGLAP evolution is expected to break down at low x. Other approaches to parton dynamics at low x include the BFKL and CCFM evolution schemes. One way to study these effects is the one proposed by Müller and Navelet, which consists of analysing the production of jets close to the proton beam direction at HERA or "forward jets".

To search for breakdown of DGLAP evolution, the ZEUS Collaboration has measured [25] forward-jet production at low x. Figure 17a shows the cross section as a function of x, together with the pQCD predictions; the measured cross section increases as x decreases. The $\mathcal{O}(\alpha_s)$ predictions are well below the data, whereas the $\mathcal{O}(\alpha_s^2)$ calculations are closer to the data, but still fall short. The $\mathcal{O}(\alpha_s^2)$ calculation is much larger than the $\mathcal{O}(\alpha_s)$ calculation and has large uncertainties; this indicates that higher orders are important. This can be understood by the opening of a new channel (gluon exchange in the t-channel) in these calculations, so that the $\mathcal{O}(\alpha_s^2)$ calculation becomes an effective LO estimation.

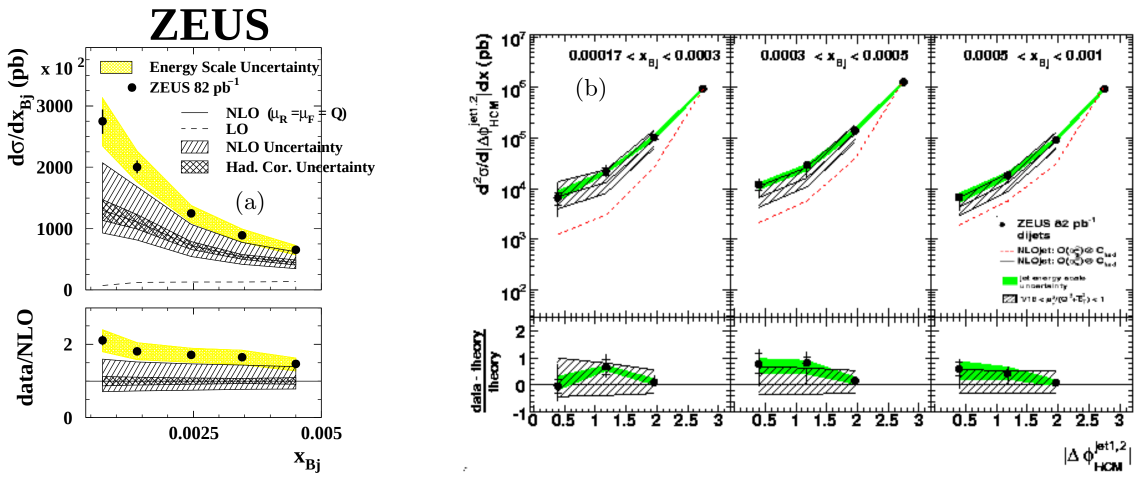

Figure 17: (a) Forward-jet cross section as a function of $x_{\rm Bj}$; (b) dijet cross sections as functions of $|\Delta\phi|$ in different $x_{\rm Bj}$ regions.

Multi-jet cross sections are better suited to test parton dynamics at low x since for dijet and three-jet cross sections a "genuine" NLO calculation can be performed. The ZEUS Collaboration has measured [26] the angular correlation as a function of $\Delta\phi$ for dijets in different regions of x (see Fig. 17b). The $\mathcal{O}(\alpha_s^2)$ calculations are one order of magnitude below the data for small jet angular separations, whereas the $\mathcal{O}(\alpha_s^3)$ calculations describe the data much better; this demonstrates the importance of the higher orders at low x. The H1 Collaboration has measured [27] the x distribution for three-jet events and for the configuration of two central jets and one forward jet (see Fig. 18). The $\mathcal{O}(\alpha_s^3)$ calculation describes the data at low x reasonably well.

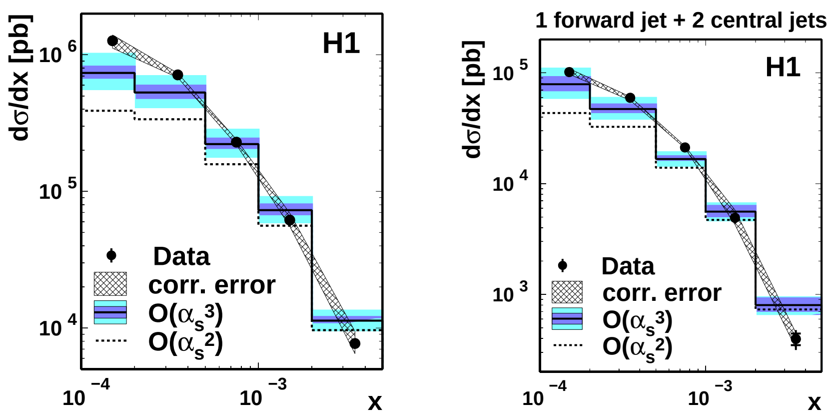

Figure 18: Three-jet cross section as a function of x for all events (left) and events with two central jets and one forward jet (right).

7. Summary and conclusions

A wealth of new measurements from HERA and TevaTron test QCD nowadays with high precision. These data probe the theory up to the highest available energies and down to the lowest possible x values, phase-space regions of special interest at LHC. The exploration of these new regimes may well lead towards a new level of understanding hard processes which will be crucial for interpreting any physics at LHC.

In particular, the underlying event has been tested in all possible environments, new high precision data will help to constrain further the proton PDFs, more and more precise determinations of the strong coupling are being obtained (see Fig. 19) and successful tests of colour dynamics at the highest available energies and down to the lowest possible

x values have been performed.

For further progress in understanding QCD and take full advantage of the available data, higher-orders corrections will be extremely useful.

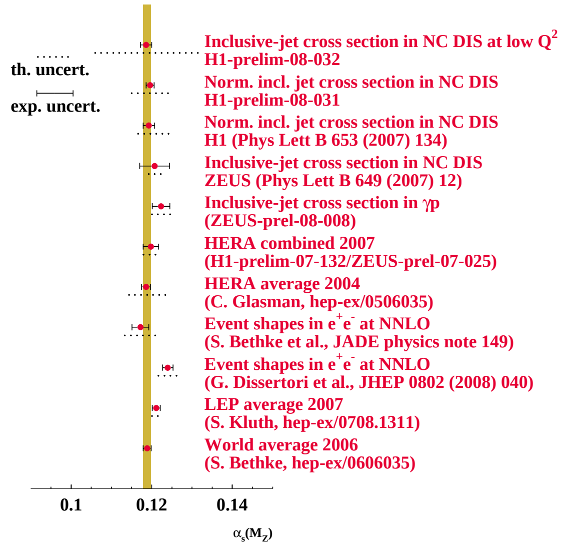

Figure 19: Summary of recent $\alpha_s(M_Z)$ determinations compared to the current world average.

Acknowledgments. I would like to thank the organisers of the ICHEP08 conference for providing me with the opportunity of giving this talk and for a well organised conference. I would like to thank C. Diaconu, G. Dissertori, K. Hatakeyama, G. Hesketh, A. Juste, S. Kluth, C. Pahl, S. Soldner-Rembold, A. Specka, J. Terrón and M. Wobisch for their help in preparing the talk. Special thanks to Prof. J. Terrón for a critical reading of this manuscript.

References

[1] CDF Coll., abstract 419, CDF/PUB/CDC/PUBLIC/9351.

[2] H1 Coll., abstract 849, H1-prelim-08-036.

[3] ZEUS Coll., abstract 130, S. Chekanov et al., *Nucl. Phys.* **B** 792 (2008) 1.

[4] CDF Coll., abstract 452, CDF/DOC/JET/PUBLIC/8928 and CDF/9246.

[5] DØ Coll., abstract 506, hep-ex/0802.2400.

[6] DØ Coll., abstract 507, Conference Note 5733-CONF.

[7] ZEUS Coll., abstract 143, ZEUS-prel-07-005.

[8] ZEUS Coll., abstract 125, S. Chekanov et al., *Phys. Rev.* **D** 76 (2007) 072011.

[9] ZEUS Coll., abstract 132, S. Chekanov et al., *Phys. Rev.* **D** 78 (2008) 032004.

[10] H1 Coll., abstract 845, H1-prelim-08-032.

[11] ZEUS Coll., abstract 121, S. Chekanov et al., *Phys. Lett.* **B** 649 (2007) 12.

[12] ZEUS Coll., abstract 152, ZEUS-prel-08-008.

[13] H1 Coll., abstract 844, H1-prelim-08-031.

[14] H1 and ZEUS Collaborations, abstract 628, H1-prelim-07-132 and ZEUS-prel-07-025.

[15] CDF Coll., abstract 411, http://www-cdf.fnal.gov/physics/new/qcd/inclpho08/web.html.

[16] DØ Coll., abstract 509, hep-ex/0804.1107.

[17] H1 Coll., abstract 846, H1-prelim-08-033.

[18] H1 Coll., abstract 797, F.D. Aaron et al., *Eur. Phys. Jour.* **C** 54 (2008) 371.

[19] CDF Coll., abstract 416, T. Aaltonen et al., *Phys. Rev.* **D** 77 (2008) 011108 and T. Aaltonen et al., *Phys. Rev. Lett.* 100 (2008) 102001.

[20] DØ Coll., abstract 604, hep-ex/0808.1296.

[21] DØ Coll., abstract 605, hep-ex/0803.2259.

[22] CDF Coll., abstract 967, T. Aaltonen et al., *Phys. Rev. Lett.* 100 (2008) 091803.

[23] CDF Coll., abstract 415, http://www-cdf.fnal.gov/physics/new/qcd/zbjet08/index.html and http://www-cdf.fnal.gov/physics/new/qcd/wbjets1900public/index.html.

[24] DØ Coll., abstract 526, Conference Note 5724-CONF.

[25] ZEUS Coll., abstract 126, S. Chekanov et al., *Eur. Phys. Jour.* **C** 52 (2007) 515.

[26] ZEUS Coll., abstract 122, S. Chekanov et al., *Nucl. Phys.* **B** 786 (2007) 152.

[27] H1 Coll., abstract 798, F.D. Aaron et al., *Eur. Phys. Jour.* **C** 54 (2008) 389.